Nonlinear Dynamics and Systems Theory, **7** (4) (2007) 409–417

# Third-Body Perturbation Using Single Averaged Model: Application to Lunisolar Perturbations

C.R.H. Solórzano and A.F.B.A. Prado *

*Instituto Nacional de Pesquisas Espaciais (INPE)*
*São José dos Campos – 12227–010 – Brazil*

Received: November 7, 2006; Revised: August 31, 2007

**Abstract:** In this paper, we considered the third-body perturbation using a single averaged model to study the effect of lunisolar perturbations on high-altitude Earth satellites. We combine two third-body perturbations. If no resonance occurs with the Moon or the Sun, short period terms are eliminated. In this way, we developed a semi-analytical study of the perturbation caused in a spacecraft by a third body with a single averaged model to eliminate the terms due to the short time periodic motion of the spacecraft. Several plots will show the time histories of the Keplerian elements.

**Keywords:** *Single averaged model; lunisolar perturbation; spacecraft.*

**Mathematics Subject Classification (2000):** 34C29, 65H05.

## 1 Introduction

The effects of the gravitational attractions of the Sun and the Moon in the orbits of an Earth's artificial satellites have been studied in several papers. Kozai [8] writes down the Lagrange's planetary equations and the disturbing function due to the Sun and to the Moon, including both secular and long periodic terms. Frick and Garber [4], using linear analysis, show that the result of the lunisolar attraction is a change of the orbital plane with small oscillations. Moreover, Musen [10] determines the long periodic disturbances caused by the Moon and the Sun in the motion of an artificial satellite. Kaula [6] derived general terms from the disturbing function for the lunisolar disturbance using equatorial elements for the Moon and the Sun.

* Corresponding author: prado@dem.inpe.br

 

Zee [16] studied the effects of the Sun and the Moon on a near-equatorial synchronous satellite, with particular attention to the trajectories of a geo-stationary synchronous satellite under the influence of the gravitational fields of an oblate Earth, the Sun and the Moon. Another work is the one by Kozai [9] that developed an alternative method for the calculation of the lunisolar disturbances. The disturbing function was expressed in terms of the orbital elements of the satellite and the geocentric coordinates of the Sun and the Moon.

Hough [5] used the Hamiltonian formed by a combination of the declination and the right ascension of the satellite, the Moon, and the Sun, and studied the periodic perigee motion for orbits near the critical inclinations $63.40^0$ and $116.60^0$. The theory predicts the existence of larger maximum fluctuations in eccentricity and faster oscillations near stable equilibrium points. Delhaise and Morbidelli [3] investigated the lunisolar effects of a geosynchronous artificial satellite orbiting near the critical inclination, analyzing each harmonic formed by a combination of the satellite and the Moon's longitude of the node. He demonstrated that the dynamics induced by these harmonics does not show resonance phenomena. Breiter [1] studied the effect in the resonance of apsides for satellites of low altitude, determining the resonant eccentricities between the secular motion of a satellite in terrestrial orbit and the longitudes of the Moon and the Sun. This study was made in hamiltonian form.

All these works present rich contributions and possess a sufficiently analytical approach, rich in derivations of equations. In the present work, an approach will be used to search numerical results, aiming to complement the existing literature. Papers more directed toward results and numerical comparisons had appeared recently, as the ones made by Broucke [2], Prado [11]. They all studied the disturbance of one third body on a satellite making an analytical and numerical study.

## 2 Mathematical Models

Our model can be formulated in a very similar way of the formulation of the planar restricted three-body problem. There are three bodies involved in the dynamics: one body with mass $m_0$, fixed in the origin of the reference system, a second massless body in orbit around $m_0$ and a third body (m') in a circular orbit around $m_0$ (see Figure 2.1). The motion of the spacecraft (the second massless body) is Keplerian and three-dimensional, with its orbital elements perturbed by the third body. The motion of the spacecraft is studied with the single averaged model, where the average is performed with respect to the true anomaly of the spacecraft (f). The disturbing function is then expanded in Legendre polynomials. The main body $m_0$ is fixed in the center of the reference system X-Y. The perturbing body m' is in a circular orbit with semi-major axis a' and mean motion n'. The spacecraft is in a three dimensional orbit, with orbital elements a, e, i, $\omega$, $\Omega$ and mean motion n. In this situation, the disturbing potential that the spacecraft has from the action of the perturbing body is given by using the expansion in Legendre polynomials and assuming that $r' \gg r$.

$$\begin{aligned} R &= \mu' G(m_0 + m')/\sqrt{r^2 + r'^2 - 2rr'\cos(S)}, \\ R &= (\mu'(m_0 + m')/r') \sum_{n=2}^{\infty} (r/r')^n P_n \cos(S). \end{aligned} \tag{1}$$

The next step is to average all there terms of the disturbing function over the short period of the satellite. The definition for average used is:

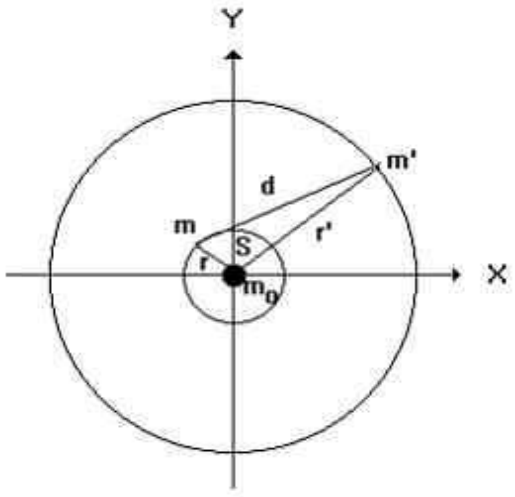


**Figure 2.1:** Illustration of the third body perturbation.

$$\langle G\rangle = (1/2)\int_0^{\infty} G dM. \tag{2}$$

Remember that M is the mean anomaly of the satellite and M' is the mean anomaly of the perturbing body. The results are made for the special case of circular orbits for the perturbing body and with the initial mean anomaly of the perturbing body equal to zero. The following relations are available (see [2]):

$$\alpha = \cos(\omega)\cos(\Omega - M') - \cos(i)\sin(\omega)\sin(\Omega - M'), \tag{3}$$

$$\beta = -\sin(\omega)\cos(\Omega - M') - \cos(i)\cos(\omega)\sin(\Omega - M'). \tag{4}$$

With those relations it is possible to relate the angle S with the positions of the perturbing and the perturbed bodies.

$$\cos(S) = \alpha\cos(f) + \beta\sin(f). \tag{5}$$

Substituting expression (5) into equation (1), and considering the equations (2)-(4), we have, after the averaged equations of motion of the spacecraft that are derived from the Lagrange's planetary equations, that they depend on the derivatives of the disturbing function [14]. It is noticed that the semi-major axis always remains constant. This occurs because, after the averaging, the disturbing function does not depend on $M_0$ (more details are available in [13]).

## 3 Results

We are now interested in the combined effects of the Moon and the Sun. For this, it is important to find the expansions of the disturbing function of the Sun and the Moon.

The term of second order due to the Sun is equivalent to the one of fourth order due to the effects of the Moon. In this section, simulations will consider the expansion made for the disturbing function of the Sun and the Moon in a combined form. The tests will be made considering satellites located in orbits with semi-major axis of 0.070 and 0.110 canonical units (26908 km and 42284 km).

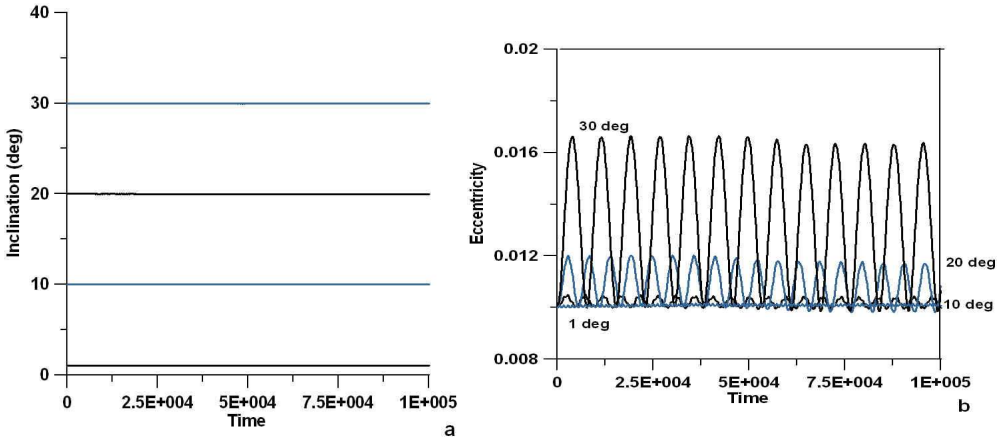


**Figure 3.1:** Behaviour of the orbital elements for values of the initial inclination below the critical value. (a) Inclination, (b) Eccentricity, both with a = 0.110.

The results for the lunisolar disturbance show a behavior similar to the ones obtained for the disturbance of the third body. Figure 3.1a shows the evolution of the inclination for initial values below the critical inclination. For the time scale used, the behavior of the inclination is constant. When analyzing the behavior of the eccentricity, it can be observed the several amplitudes reached with the increment of the initial inclination (Figure 3.1b). For an initial value of the inclination of 30 degrees, the eccentricity presents an amplitude around of 0.006, and for an initial inclination of 20 degrees, the eccentricity has an amplitude of 0.002. These small values do not change too much the orbit, since they still remain as almost-circular.

For larger values of the initial inclination (above the critical value), there is a typical behavior. It initiates in its initial value and soon it goes down until the critical value (Figure 3.2a) and then returns to the initial value. This oscillatory behavior presents the characteristic that, as the initial inclination increases, the amplitude of the inclination suffer increases. This fact reflects in the evolution of the eccentricity (Figure 3.2b), where the orbits with small eccentricities (almost circular) reach high values for the eccentricities, what affects the stability of the near-circular orbits. When the inclination reaches its minimum value, the eccentricity reaches its maximum value. This repetitive behavior is shown the Figures 3.2a and 3.2b, where the inclination starts in its initial value and, after a certain period, the inclination goes to its minimum value and the eccentricity reaches its maximum value.

For values of the inclination near the critical one (around 40°), we observe that, for values smaller than the critical inclination, there is an almost constant variation

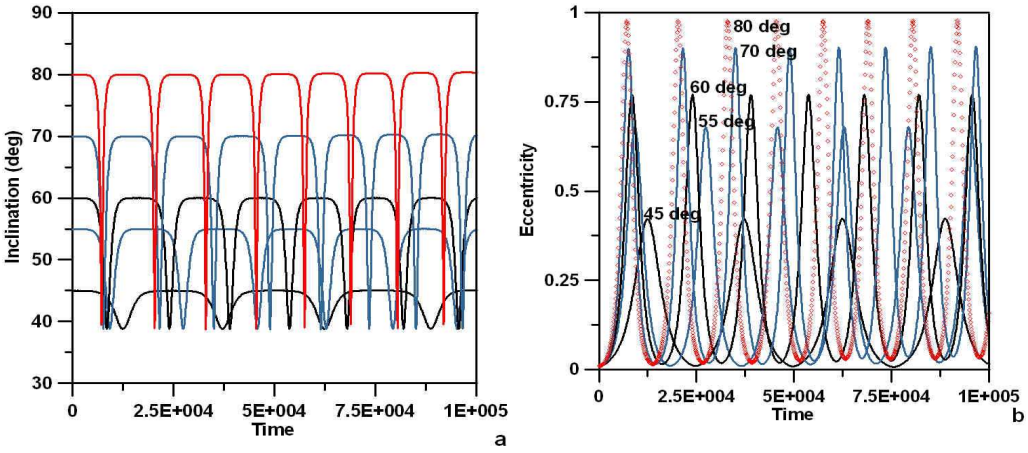


**Figure 3.2:** Behaviour of the orbital elements for values of the initial inclination above the critical value. (a) Inclination, (b) Eccentricity, both with a = 0.110.

(Figure 3.3a). As this value suffer increases, the inclination variations become larger. In the analysis of the eccentricity (Figure 3.3b), we observe that a zone exists where the eccentricity presents small oscillations. However, there are regions where it suffers large variations, making the almost circular orbit a very elliptical one. Figure 3.3c shows the evolution of the argument of the pericenter for values of the initial inclination near the critical value. The figures show the secular behavior of the argument of the pericenter for the time scale used. For larger times, it is observed the phenomenon called circulation. For an interval of shorter times, the secular curves are formed by small oscillations. Moreover, Figure 3.3d illustrates the retrograde behavior of the longitude of the node.

For an orbit with semi-major axis of 0.07 canonical units, one of the main characteristics is the small number of oscillations per unit of time. This brings, as a consequence, that when the satellite is located in a orbit with a semi-major axis of 0.110 canonical units, it reaches the critical inclination quickly. In Figure 3.5a we observe that, for initial inclination of 45 degrees, the satellite reaches its first critical value for a time of 25000 canonical units. In Figure 3.2a it is observed that the orbit reaches the critical inclination near 12000 canonical units of time. In the evolution of the inclination and the eccentricity, for the values of the initial inclination below the critical value, the inclination (Figure 3.4a) keeps its typical behavior, even that the eccentricity does not change significantly. As a consequence of that, the time necessary to reach the critical inclination is larger, and the number of oscillations in the evolution of the eccentricity is smaller (Figure 3.4b and Figure 3.5b). So, the analyzed behavior shows that, with high eccentricities, smaller inclinations are reached, as can be seen in the previous figures.

The evolution of the argument of the pericenter for initial inclinations larger than the critical value has secular and oscillatory behavior. It is an interesting point that, as the initial inclination increases, the satellite reaches higher values for the argument of the perigee. In the case of the longitude of the node, it presents the secular and

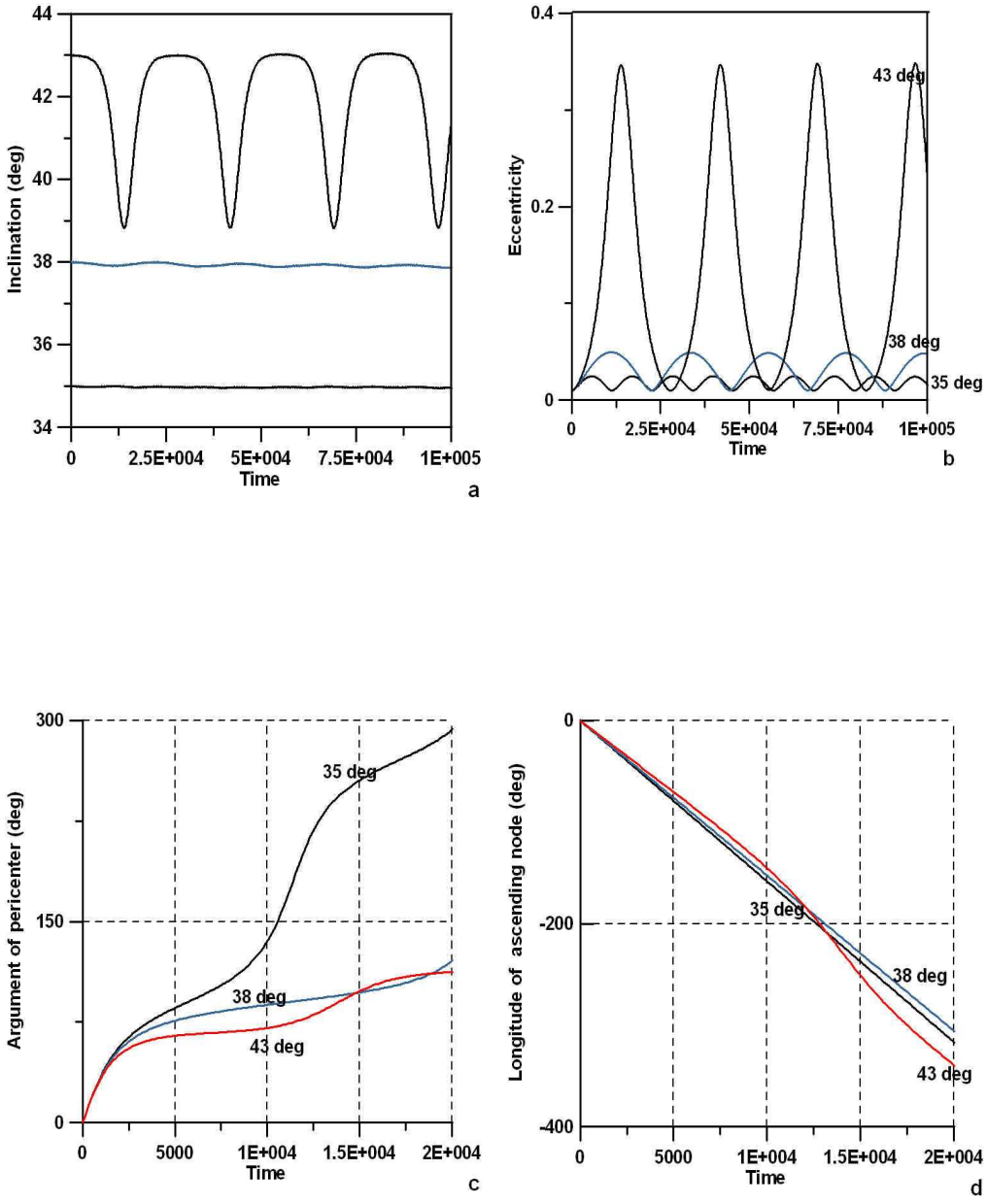


**Figure 3.3:** Behaviour of the orbital elements for values of the initial inclination near of critical value (a=0.110).

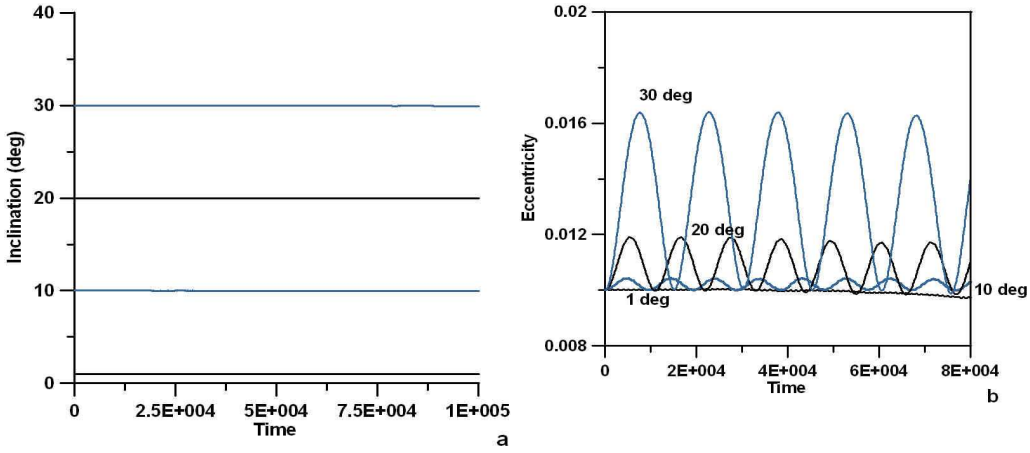


**Figure 3.4:** Behaviour of the orbital elements for values of the initial inclination below the critical value. (a) Inclination, (b) Eccentricity, both with a = 0.07.

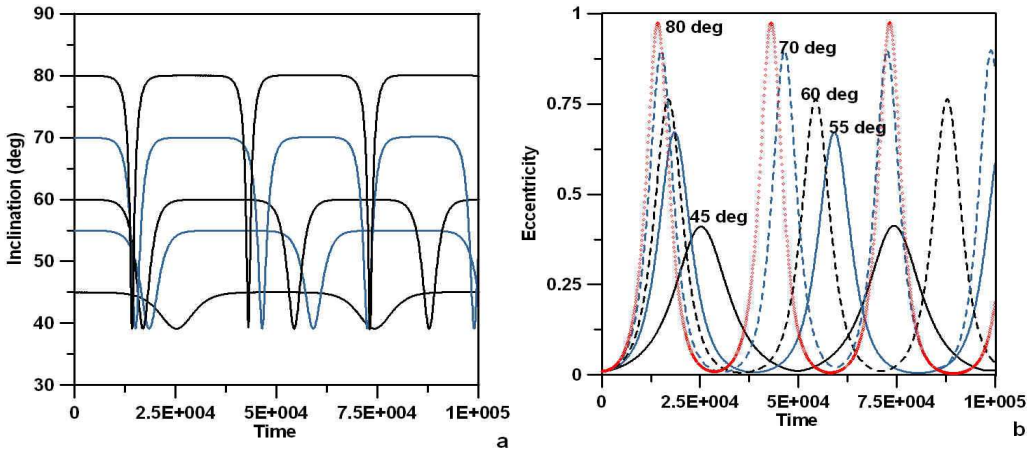


**Figure 3.5:** Behaviour of the orbital elements for values of the initial inclination above the critical value. (a) Inclination, (b) Eccentricity, both with a = 0.07.

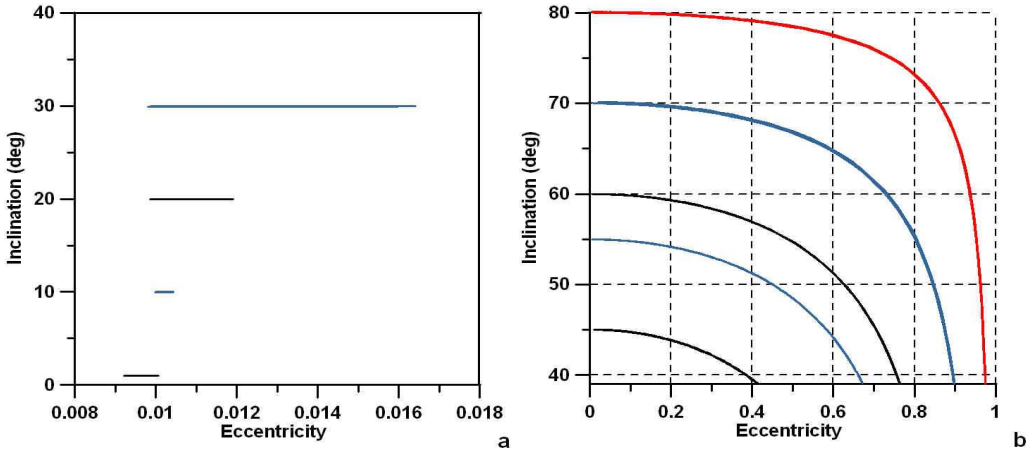


**Figure 3.6:** Eccentricity vs. inclination for several initial inclination. (a) Initial inclination below the critical value, (b) Initial inclination above the critical value, both with a = 0.07.

retrograde typical behavior. Figure 3.6 shows the behavior of the inclination and the eccentricity. For values of the inclination smaller than the critical value, there are small variations in the inclination and the eccentricity. These small oscillations allow that the almost circular orbits remain almost circular, but when the initial inclinations increase, the amplitude become larger.

## 4 Conclusions

Broucke [2] and Prado [11] used the approach of double-averaging technique to develop semi-analytical methods for the third-body perturbation. In another work, Solórzano et al [12] determined the effect of the disturbance of the third body by means of the single averaged model, being dedicated to the perturbative effects of the Moon in a spacecraft, but it did not considerer the case of lunisolar perturbation. When considering the disturbance of the third body by means of the single averaged model for the combined effect of the Sun and the Moon, in particular when the values of the initial inclination are below the critical value, the near-circular orbits remain near-circular. However, for values of the initial inclination above this value, the near-circular orbits become highly elliptical. This fact causes serious problems for the the stability of these orbits, being able to cause the collision of a spacecraft with the mother planet or the expulsion of the spacecraft of the orbit around the primary. All the results are a demonstration of the Kozai resonance. Our solution to the problem take terms of up to second-order in the expansion of the Sun's disturbing function and the fourth-order in the expansion of the Moon's disturbing function. The orbits of both (Sun and Moon) are considered as circular and coplanar. The critical angle of the disturbance of the third body appears of similar form to the critical angle obtained for the perturbative effects of the oblatenesses of the Earth on the spacecraft. However, other works as Kinoshita and Nakai [7] and

Yokoyama [15] make an estimate of the critical semi-major axis, as being the distance to which the effect of the oblatenesses and the solar disturbance are equivalent.

## Acknowledgments

The authors are grateful to CAPES (Coordenação de Aperfeiçoamento de Pessoal de Nível Superior), to the São Paulo State Science Foundation (FAPESP) for the research grant received under Contract 2003/03262-4 and to CNPq (Brazilian National Council for Scientific and Technological Development) for the contract 300221/95-9.

## References

[1] Breiter, S. Lunisolar apsidal resonances at low satellite orbits. *Celestial Mechanics and Dynamical Astronomy* **74** (1999) 253–274.

[2] Broucke, R.A. Long-term third body effects via double averaging. *Journal of Guidance Control and Dynamics* **25**(1) (2003) 27–32.

[3] Delhaise, F. and Morbidelli, A. Lunisolar effects of Geosynchronous orbits at the critical inclination. *Celestial Mechanics and Dynamical Astronomy* **57** (1993) 155–173.

[4] Frick, R.H. and Garber, T.B. Perturbations of synchronous satellites. *Rand Corp. Report NASA* **399** (1962), 186 p.

[5] Hough, M.E. Lunisolar perturbations. *Celestial Mechanics and Dynamical Astronomy* **25** (1981) 111–136.

[6] Kaula, W.M. Development of the lunar and solar disturbing functions for a close satellite. *The Astronomical Journal* **67**(5) (1962) 300–303.

[7] Kinoshita, H. and Nakai, H. Secular perturbation of fictitious satellites of Uranus. *Celestial Mechanics and Dynamical Astronomy* **52** (1991) 293–303.

[8] Kozai, Y. On the effects of the Sun and Moon upon the motion of a close Earth satellite. *Smithsonian Inst. Astrophysical Observatory* **6** (1963), 47 p.

[9] Kozai, Y. A new method to compute lunisolar perturbations in satellite motions. *Smithsonian Inst. Astrophysical Observatory* **349** (1973) 27 p.

[10] Musen, P. On the long-period lunar and solar effect on the motion of an artificial satellite. *Journal of Geophysical Research* **66** (1961) 2797–2813.

[11] Prado, A.F.B.A. Third-body perturbation in orbits around natural satellites. *Journal of Guidance, Control and Dynamics* **26**(1) (2003) 33–40.

[12] Solórzano, C.R.H., Prado, A.F.B.A. and Kuga, H.K. Third-body perturbation using a single averaged model. *Proc. of the 16th Int. Symposium on Space Flight Dynamics*. Pasadena, California, EE.UU, 2001, 9 p.

[13] Solórzano, C.R.H. *Third-body perturbation using a single averaged model*. Master Dissertation, National Institute for Space Research (INPE), São José dos Campos, SP, Brazil, 2002.

[14] Taff, L.G. *Celestial Mechanics*. A Wiley – Interscience Publication (1985).

[15] Yokoyama, T. Dynamics of some fictitious satellites of Venus and Mars. *Planetary and SpaceScience* **47** (1999) 619–617.

[16] Zee, C. H. Effects of the Sun and the Moon on a near-equatorial synchronous satellite. *Astronautica Acta* **17** (1972) 891–906.